Available online at www.sciencedirect.com
ScienceDirect
Journal of Molecular Catalysis A: Chemical 281 (2008) 59–65
JOURNAL OF MOLECULAR CATALYSIS A: CHEMICAL
www.elsevier.com/locate/molcata

Water–gas shift activity of Au and Cu nanoparticles supported on molybdenum oxides

J.A. Rodríguez [a,*], P. Liu [a], J. Hrbek [a], M. Pérez [b], J. Evans [b]

[a] *Chemistry Department, Brookhaven National Laboratory, Upton, NY 11973, USA*
[b] *Facultad de Ciencias, Universidad Central de Venezuela, Caracas 1020-A, Venezuela*

Available online 22 July 2007

Abstract

The water–gas shift (WGS, $CO + H_2O \rightarrow H_2 + CO_2$) reaction was studied on a series of gold/molybdena and copper/molybdena surfaces. Films of MoO_2 were grown by exposing a Mo(1 1 0) substrate to NO_2 at 1000 K. Then, Au and Cu nanoparticles were deposited on the oxide surfaces and their WGS activity was measured in a reaction cell ($P_{CO} = 20$ Torr; $P_{H_2O} = 10$ Torr; $T = 575$–650 K). Although bulk metallic Au is inactive as a catalyst for the WGS and worthless in this respect when compared to bulk metallic Cu, Au nanoparticles supported on MoO_2 are a little bit better catalysts than Cu nanoparticles. The WGS activity of the Au and Cu nanoparticles supported on MoO_2 is five to eight times larger than that of Cu(1 0 0). The apparent activation energies are 7.2 kcal/mol for Au/MoO_2, 7.8 kcal/mol for Cu/MoO_2, and 15.2 kcal/mol for Cu(1 0 0). The Cu/MoO_2 surfaces have a catalytic activity comparable to that of Cu/CeO_2(1 1 1) surfaces and superior to that of Cu/ZnO(0 0 0 $\bar{1}$) surfaces. Post-reaction surface characterization indicates that the admetals in Au/MoO_2 and Cu/MoO_2 remain in a metallic state, while there is a minor $MoO_2 \rightarrow MoO_3$ transformation. Formate- and/or carbonate-like species are present on the surface of the catalysts. DFT calculations indicate that the oxide support in Au/MoO_2 and Cu/MoO_2 is directly involved in the WGS process.

Keywords: Copper; Gold; Molybdenum oxides; Carbon monoxide; Hydrogen production; Water; Water–gas shift; CO oxidation

1. Introduction

This article reviews a series of studies examining the water–gas shift activity of gold and copper nanoparticles in contact with surfaces of MoO_2. Currently, the primary source of hydrogen is by steam reforming from hydrocarbons: $C_nH_m + nH_2O \rightarrow nCO + (n - m/2)H_2$. The reformed fuel contains 1–10% CO, which degrades the performance of the Pt electrode used in fuel cell systems. The water–gas shift reaction (WGS, $CO + H_2O \rightarrow H_2 + CO_2$) is critical for providing clean hydrogen [1,2]. Recent works report that Au nanoparticles supported on oxides (CeO_2, ZnO, TiO_2) are very efficient catalysts for the WGS reaction [2–5]. Bulk metallic gold typically exhibits a very low chemical and catalytic activity [1,6]. Among the transition metals, gold is by far the least reactive [6], and is often referred to as the "coinage metal". In the last 10 years, gold has become the subject of a lot of attention due to its unusual catalytic properties when dispersed on some oxide supports [7–16]. Several models have been proposed for explaining the activation of supported gold: from special chemical properties resulting from the limited size of the active gold particles (usually less than 10 nm), to the effects of metal ↔ support interactions (i.e. charge transfer between the oxide and gold) [4,5,7–9,12–14]. In principle, the active sites for the catalytic reactions could be located only on the supported Au particles or on the perimeter of the gold–oxide interface [4,5,7,12]. In this article, we investigate the WGS activity of the Au/MoO_2 system. MoO_2 is interesting as an oxide support because its Mo cations are not fully oxidized and could participate in different steps of the WGS reaction.

The second system under study here is Cu/MoO_2. Copper supported on ZnO is perhaps the most common WGS catalyst used in the industry [1,2]. The Cu–ZnO system is pyrophoric and normally requires lengthy and complex activation steps before usage [17]. Consequently other catalysts are being sought. Recently, a novel and active Cu–MoO_2 catalyst was synthesized by partial reduction of a $CuMoO_4$ precursor with CO or H_2 at 200–250 °C [18]. The phase transformations were followed using *in situ* time-resolved X-ray diffraction. During the reduction process the diffraction pattern of the $CuMoO_4$ collapsed and copper metal lines were observed on an amorphous

* Corresponding author. Tel.: +1 631 344 2246; fax: +1 631 344 5815.
E-mail address: rodrigez@bnl.gov (J.A. Rodríguez).

1381-1169/$ – see front matter © 2007 Elsevier B.V. All rights reserved.
doi:10.1016/j.molcata.2007.07.032

background that was assigned to molybdenum oxides. Under WGS reaction conditions, diffraction lines for $Cu_6Mo_5O_{18}$ and MoO_2 appeared around 350 °C and $Cu_6Mo_5O_{18}$ was further transformed to Cu/MoO_2 at higher temperature. Significant WGS catalytic activity was observed with relatively stable plateaus in product formation around 350, 400 and 500 °C [18]. There is a need to study this system in more detail to establish the relative importance of interfacial interactions between Cu particles and the MoO_2 support [18].

In this work, we investigated the WGS reaction on Cu and Au nanoparticles supported on polycrystalline films of MoO_2 growth on a Mo(1 1 0) substrate [19]. The surfaces are prepared and characterized in an ultra-high vacuum chamber and their catalytic activity is tested in an attached high-pressure reactor. In previous studies this approach proved to be very useful for studying the kinetics and mechanism of the WGS reaction on copper surfaces [20–22], and on Cu and Au nanoparticles supported on CeO_2(1 1 1) and ZnO(0 0 0 $\bar{1}$) [4]. One of our objectives here is to establish patterns of reactivity as a function of the admetal coverage and oxide support.

2. Experimental and theoretical methods

2.1. Catalyst preparation and activity

The experiments were performed in an ultrahigh-vacuum (UHV) chamber that has attached a high-pressure cell or batch reactor [4,10]. The sample could be transferred between the reactor and vacuum chamber without exposure to air. The UHV chamber (base pressure $\sim 5 \times 10^{-10}$ Torr) was equipped with instrumentation for X-ray photoelectron spectroscopy (XPS), low-energy electron diffraction (LEED), ion scattering spectroscopy (ISS), and thermal-desorption mass spectroscopy (TDS).

Polycrystalline films of MoO_2 were prepared by exposing a Mo(1 1 0) surface to NO_2 at 1000 K [19]. The surface was oxidized by the reaction: $NO_{2,gas} \rightarrow O_{ads} + NO_{gas}$. A typical Mo 3d XPS spectrum obtained after this process is shown in Fig. 1.

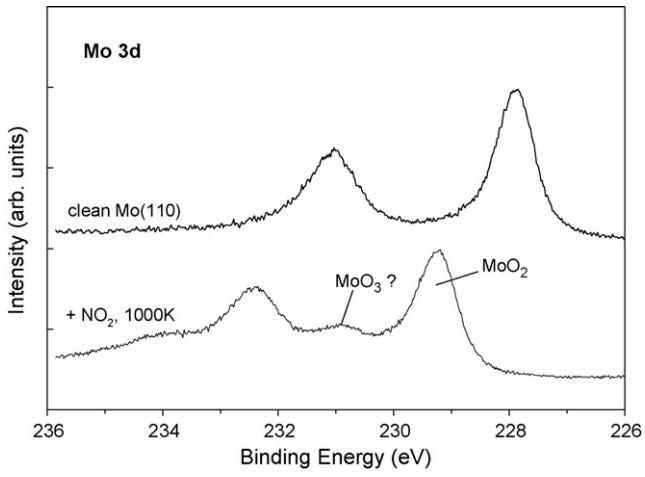

Fig. 1. Mo 3d spectra acquired before and after dosing NO_2 to a Mo(1 1 0) substrate at 1000 K.

The dosing of NO_2 leads to a complete disappearance of the $3d_{5/2}$ peak for metallic Mo and a strong new feature appears at ~229.3 eV. This feature is shifted ~1.5 eV with respect to metallic Mo and indicates the formation of a multilayer of MoO_2 [23]. The spectrum for the oxide film exhibits secondary features that could be due to a small amount of MoO_3 [19,23]. The relative ratio of MoO_3/MoO_2 depended on the magnitude of the NO_2 dose. In general, we worked with oxide films that were very rich in MoO_2. Cu and Au were vapour deposited on the molybdenum oxide films at room temperature [4,10], and then the sample was heated to the WGS reaction temperature (575–650 K). The flux from the metal dosers was calibrated by depositing Cu or Au on the clean Mo(1 1 0) crystal and taking TDS spectra of the admetals [4,10]. ISS indicates that Cu and Au grow on MoO_2 forming three-dimensional islands as seen on CeO_2(1 1 1), ZnO(0 0 0 $\bar{1}$) or TiO_2(1 1 0) [4,7,11]. After each experiment with the Cu/MoO_2 or Au/MoO_2 surfaces, the Mo(1 1 0) substrate was cleaned by e-beam heating it to 2200 K.

In the kinetic measurements the sample was transferred to the batch reactor at ~300 K, then the reactant gases were introduced (20 Torr of CO and 10 Torr of H_2O) and the sample was rapidly heated to the reaction temperature (575, 600, 625 or 650 K). The CO gas was cleaned of any metal carbonyl impurity by passing it through purification traps. Product yields were analyzed by a gas chromatograph [4,21]. The amount of molecules produced was normalized by the active area exposed by the sample. The sample holder was passivated by extensive sulphur poisoning (exposure to H_2S) and have no catalytic activity. In our reactor a steady-state regime for the production of H_2 and CO_2 was reached after 2–3 min of reaction time. The kinetic experiments were done in the limit of low conversion (<5%).

2.2. Density functional calculations

The unrestricted density-functional (DF) calculations were performed with the DMol^3 code, using effective core potentials, a numerical basis set, and the GGA-PW91 description of the exchange and correlation functionals [24,25]. Transition states here were identified using the combination of synchronous transit methods and eigenvector following, and verified by the presence of a single imaginary frequency from a sequential vibrational frequency analysis. Cu(1 0 0) and Au(1 1 1) were modelled using four-layer slabs [26]. During the DF calculations the geometries of the top two layers of the slabs and the Cu or Au nanoparticles were fully relaxed.

3. Results and discussion

3.1. The water–gas shift reaction on copper/molybdena surfaces

Fig. 2 shows the WGS activity of model Cu/MoO_2 catalysts as a function of admetal coverage. The pure films of molybdenum oxide displayed no activity for the WGS under the reaction conditions investigated here. Upon adding

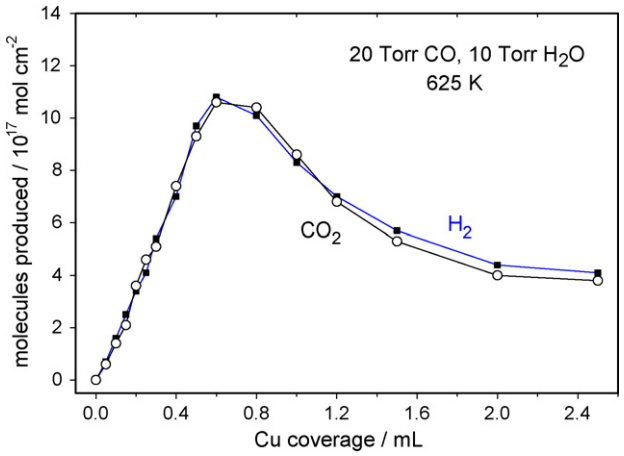

Fig. 2. WGS activity of model Cu/MoO_2 catalysts as a function of admetal coverage. Each surface was exposed to a mixture of 20 Torr of CO and 10 Torr of H_2O at 625 K for 5 min. Steady-state was reached 2–3 min after introducing the gases in the batch reactor.

Cu to MoO_2, there is a continuous increase in the catalytic activity until a maximum is reached at coverages of 0.6–0.8 ML. After this point, the production of H_2 and CO_2 starts to decrease. This trend can be attributed to a decrease in catalytic activity when the Cu particle size becomes very large [4,5]. A similar phenomenon has been seen for the $Cu/CeO_2(1\,1\,1)$ and $Cu/ZnO(0\,0\,0\,\bar{1})$ surfaces [4].

Fig. 3 compares the amount of H_2 produced under similar conditions (20 Torr of CO, 10 Torr of H_2O, 625 K, 5 min) on $Cu(1\,0\,0)$ and on 0.5 ML of Cu supported over $ZnO(0\,0\,0\,\bar{1})$ [4], $CeO_2(1\,1\,1)$ [4] and MoO_2. The WGS activity seen for $Cu(1\,0\,0)$ is comparable to that detected for $Cu(1\,1\,1)$ or $Cu(1\,1\,0)$ [20,21], with variations in reactivity that are probably a consequence of changes in the structure of the copper surfaces [21]. The deposition of Cu nanoparticles on $ZnO(0\,0\,0\,\bar{1})$ produces a catalyst that is clearly more active than the pure extended Cu surfaces [4]. An even better catalyst is obtained when the nanoparticles are supported on $CeO_2(1\,1\,1)$ or MoO_2. In the case of MoO_2, the roughness of the oxide film may facilitate the reaction [10], but in any case it is likely that MoO_2 is more active as a support than ZnO.

Experiments similar to those in Fig. 3 were also done at temperatures of 575, 600 and 650 K. Again the Cu/MoO_2 system displayed an excellent performance. Using the ln of the reaction rates we constructed Arrhenius plots for the different surfaces. Fig. 4 summarizes the results for several Cu-based catalysts. The differences in catalytic activity are very pronounced at 575 K and become smaller at 650 K, but Cu/MoO_2 is always a very good catalyst. On $Cu(1\,0\,0)$ the apparent activation energy given by the slope of the Arrhenius plot is 15.2 kcal mol^{-1}. It is somewhat smaller than the value of 17 kcal mol^{-1} reported for the WGS on a $Cu(1\,1\,1)$ surface [21]. The apparent activation energy decreases to 12.4 kcal mol^{-1} on $Cu/ZnO(0\,0\,0\,\bar{1})$ [4], 8.6 kcal mol^{-1} on $Cu/CeO_2(1\,1\,1)$ [4], and 7.8 kcal mol^{-1} on Cu/MoO_2.

The kinetic data in Fig. 2 were collected using a reaction cell attached to an ultra-high vacuum chamber for surface characterization. The gases were pumped out from the reaction cell and the surfaces were post-characterized using standard XPS. In the C 1s region we found the typical peaks for adsorbed formate- or carbonate-like species proposed as intermediates in the WGS reaction [4,5]. The corresponding Cu 2p core-level and L_3VV Auger spectra indicated that copper remained in a metallic state [23]. The Mo 3d core-level spectra pointed to a minor $MoO_2 \rightarrow MoO_3$ transformation. A typical result is shown in Fig. 5. After the WGS reaction, there is an attenuation of the Mo 3d signal (probably as a consequence of the formation of HCOO or CO_x species on the oxide surface) and a decrease in the ratio of intensities for the MoO_2/MoO_3 features.

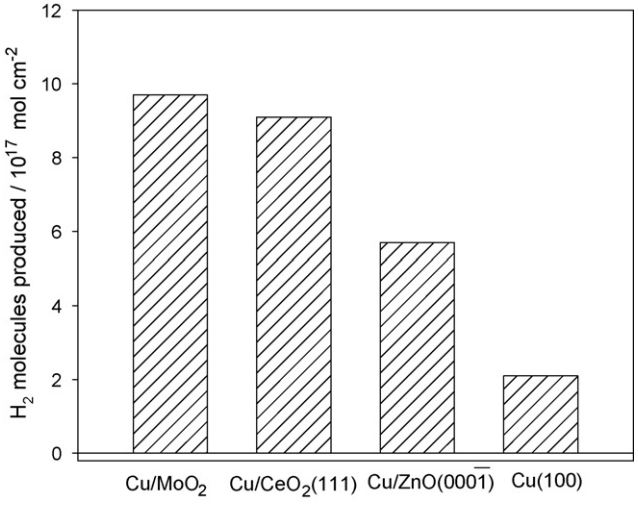

Fig. 3. H_2 produced under similar conditions (20 Torr of CO, 10 Torr of H_2O, 625 K, 5 min) on $Cu(1\,0\,0)$ and on 0.5 ML of Cu supported over $ZnO(0\,0\,0\,\bar{1})$ [4], $CeO_2(1\,1\,1)$ [4] and MoO_2.

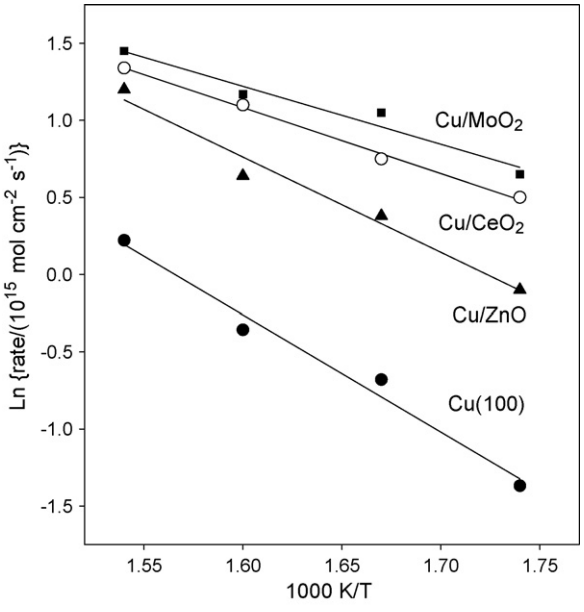

Fig. 4. The WGS reaction rate *vs*. temperature, in Arrhenius form, for $Cu(1\,0\,0)$, 0.5 ML of Cu on $ZnO(0\,0\,0\,\bar{1})$, $CeO_2(1\,1\,1)$ or MoO_2. The data were acquired with a pressure of 20 Torr of CO and 10 Torr of H_2O in a batch reactor.

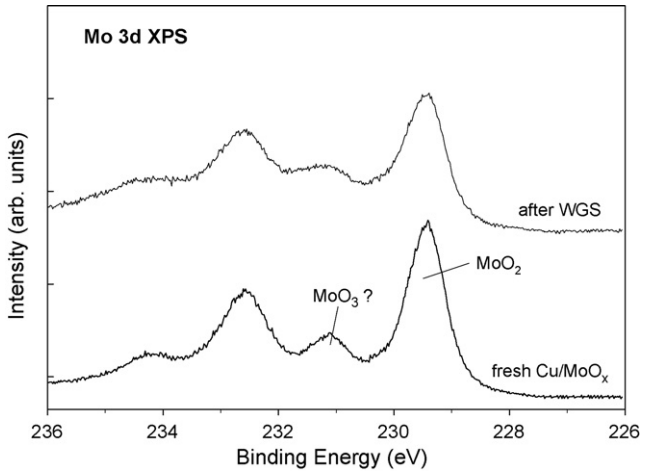

Fig. 5. Mo 3d XPS core-level spectra acquired before and after carrying-out the WGS reaction on a Cu/MoO_2 surface (Θ_{Cu} = 0.5 ML, 20 Torr of CO, 10 Torr of H_2O, 625 K, 5 min).

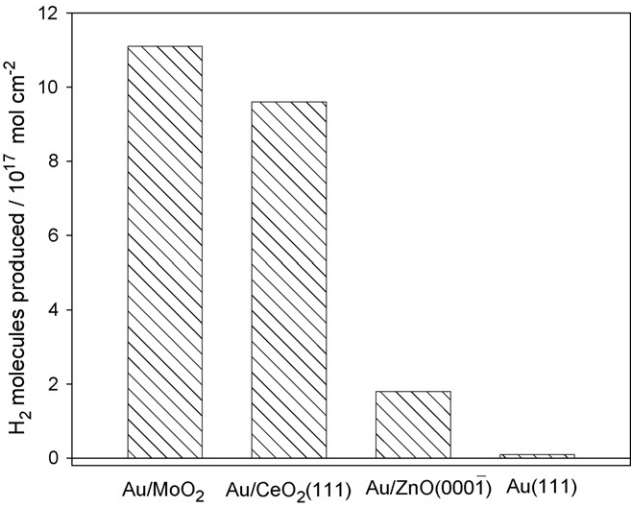

Fig. 7. WGS activity of Au(1 1 1) and 0.5 ML of Au supported on ZnO(0 0 0 $\bar{1}$) [4], CeO_2(1 1 1) [4] and a MoO_2 film (20 Torr of CO, 10 Torr of H_2O, 625 K, 5 min).

3.2. The water–gas shift reaction on gold/molybdena surfaces

In the cases of Au(1 1 1) or polycrystalline Au, we found negligible activity for the WGS [10]. Fig. 6 displays the WGS activity of Au/MoO_2 catalysts as a function of Au coverage. In contrast to the bulk surfaces of gold, the Au nanoparticles in contact with molybdena are extremely active for the WGS reaction. The maximum activity is seen at Au coverages of 0.4–0.5 ML. For Au coverages above 2 ML, the catalytic activity is considerably smaller. Such trend that has been seen for many gold/oxide catalysts [4,7,8] and has been attributed to size effects.

The WGS activity of Au(1 1 1) and 0.5 ML of Au supported on ZnO(0 0 0 $\bar{1}$) [4], CeO_2(1 1 1) [4] and a MoO_2 film is shown in Fig. 7 (20 Torr of CO, 10 Torr of H_2O, 625 K). The nature of the support plays a key role in the activation of the gold nanoparticles. Zinc oxide is frequently used in industrial Cu–ZnO WGS

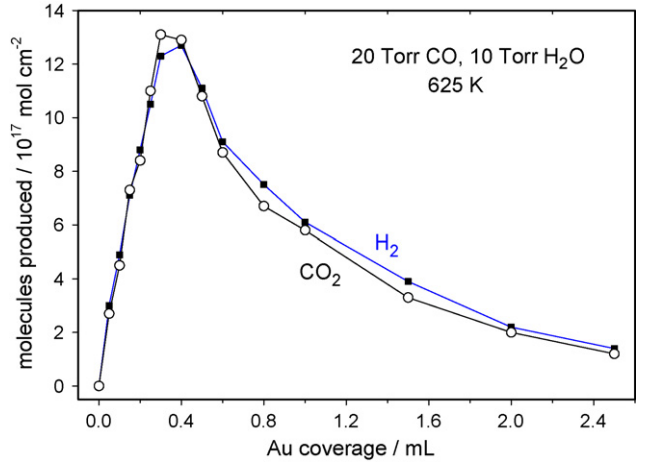

Fig. 6. WGS activity of model Au/MoO_2 catalysts as a function of admetal coverage. Each surface was exposed to a mixture of 20 Torr of CO and 10 Torr of H_2O at 625 K for 5 min. Steady-state was reached 2–3 min after introducing the gases in the batch reactor.

catalysts [1]. However, the Au/ZnO(0 0 0 $\bar{1}$) system displays low WGS activity when compared to Au/CeO_2(1 1 1) or Au/MoO_2. The ceria and molybdena oxides contain a substantial number of metal cations that are not fully oxidized under WGS reaction conditions and may participate directly in important steps of the process (see below). This is not the case for Au/ZnO(0 0 0 $\bar{1}$) [4]. Our previous work for Au on CeO_2(1 1 1) and on polycrystalline CeO_2 [10] has shown that the roughness of the surface is an important factor for catalytic activity, but cannot be invoked to explain the trends seen in Fig. 7. Post-reaction surface analysis for the Au/MoO_2 systems showed that most of the Mo cations were in a +4 formal oxidation state with only a minor $MoO_2 \rightarrow MoO_3$ transformation induced by the reaction (similar to the case of Cu/MoO_2 seen in Fig. 5).

The gold atoms in the Au/MoO_2 catalysts were probably not oxidized during the WGS process. After reaction, in XPS we found Au 4f positions that were almost identical to those seen upon deposition of the metal on MoO_2 and very different from those typical of AuO_x species [3,10]. Post-reaction surface analysis also showed the presence of formate- and/or carbonate-like groups on the surface of the catalyst. Possible reaction paths for the formation of these groups are presented in Ref. [5]. It is not completely clear if they are key intermediates in the WGS process or simple spectators [5,27,28].

Fig. 8 displays the apparent activation energies observed for 0.5 ML of Au or Cu deposited on ZnO(0 0 0 $\bar{1}$), CeO_2(1 1 1) and MoO_2. All the reported values were obtained from Arrhenius plots that contained reaction rates measured at 575, 600, 625 and 650 K under steady state conditions at P_{CO} = 20 Torr and P_{H_2O} = 10 Torr. The most active catalysts have apparent activation energies in the range of 7–9 kcal/mol, while the corresponding values for the least active catalysts are 15–16 kcal/mol. Although bulk metallic Au is inactive as a catalyst for the WGS and worthless in this respect when compared to bulk metallic Cu, Au nanoparticles supported on CeO_2 or MoO_2 are a little bit better catalysts than Cu nanoparticles.

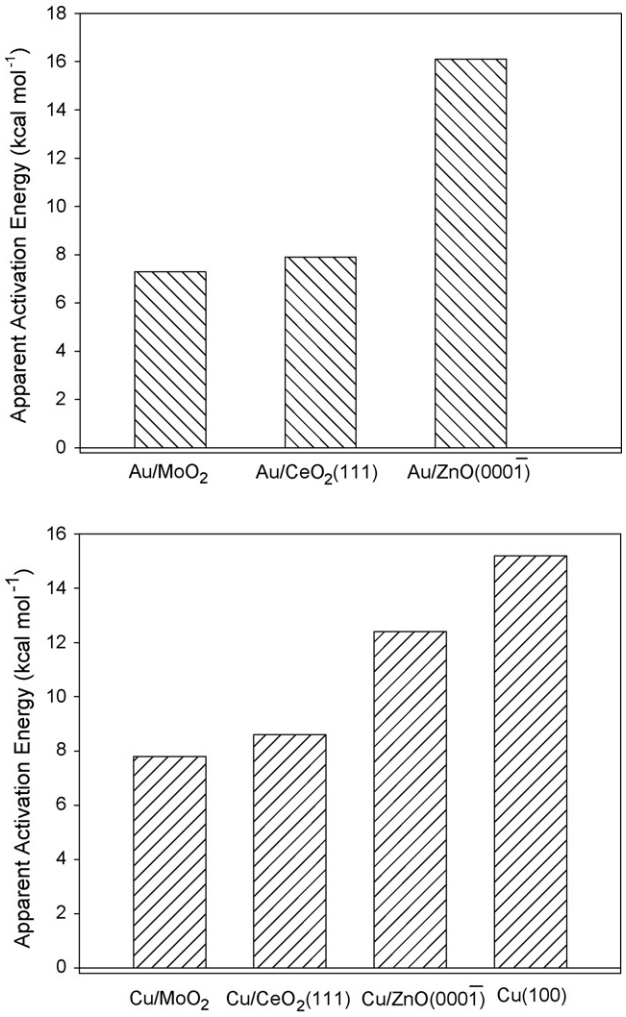

Fig. 8. Apparent activation energies observed for the WGS over 0.5 ML of Au or Cu deposited on ZnO(0 0 0 $\bar{1}$) [4], CeO_2(1 1 1) [4], and MoO_2. P_{CO} = 20 Torr, P_{H_2O} = 10 Torr.

3.3. Density-functional studies of the WGS reaction

A very important issue is to establish the intrinsic chemical activity of Cu and Au nanoparticles. Can nanoparticles of Cu and Au catalyze the WGS reaction on their own without the aid of an oxide support? Are these nanoparticles more reactive than extended surfaces of the pure metals? Theoretical studies have shown that unsupported Au nanoparticles can be very active for the oxidation of CO or the dissociation of H_2 [24]. On the other hand, results of density-functional (DF) calculations indicate that free Au clusters are not able to dissociate SO_2 [16]. Using DF calculations we investigated the WGS reaction on Cu_{29} and Au_{29} clusters, and on Cu(1 0 0) and Au(1 0 0) surfaces [7]. The Cu_{29} and Au_{29} clusters exhibited a pyramidal structure formed by the interconnection of (1 1 1) and (1 0 0) faces of the bulk metals, see Fig. 9. It has three layers containing 16, 9 and 4 metal atoms. Similar Au clusters have been observed on CeO_2 or TiO_2 with STM [24]. Our calculations indicate that an Au_{29} cluster interacts well with atomic and molecular hydrogen [24]. However, it does not bond or dissociate the water molecule. We

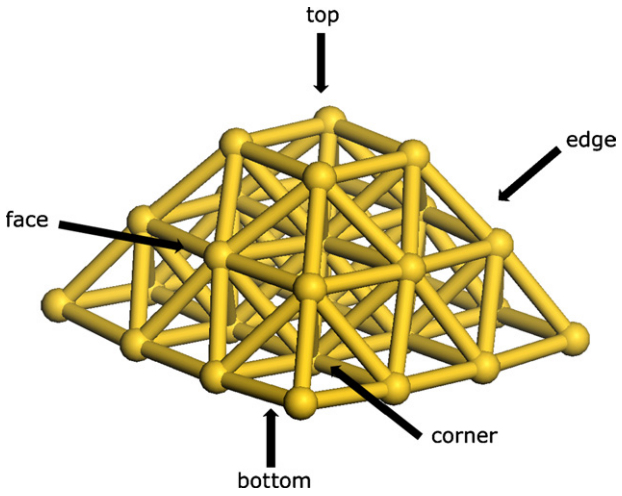

Fig. 9. Au_{29} or Cu_{29} cluster used to investigate the bonding/dissociation of a water molecule and the WGS reaction. The arrows point to the possible adsorption sites for the interaction with water.

investigated the $H_2O \leftrightarrow Au_{29}$ interactions for all the adsorption sites shown in Fig. 9 and in all cases we found no bonding. This can be contrasted with the case of a Cu_{29} cluster or a Cu(1 0 0) surface where the WGS reaction occurs readily.

Fig. 10 shows a correlation between the calculated barrier (*y*-axis) and the calculated reaction energy (*x*-axis) for water dissociation on Au(1 0 0), Cu(1 0 0) as well as ionic and neutral Au_{29} and Cu_{29} nanoparticles [4]. All the gold systems are characterized by a large activation barrier and an endothermic ΔE. When going from Au(1 0 0) to Au_{29} there is a significant improvement in chemical reactivity [25], but it is not enough for dissociating the water molecule. Charging of the Au nanoparticle to form either Au_{29}^- or Au_{29}^+ also does not help. These results cannot explain the large catalytic activity seen for Au/MoO_2 or Au/CeO_2(1 1 1) surfaces in Fig. 7. They highlight the important role of ceria or molybdena in the activation of the gold systems.

Fig. 11 shows the calculated energy profile for the WGS on periodic Cu(1 0 0) and Au(1 0 0) surfaces. On Cu(1 0 0), the first

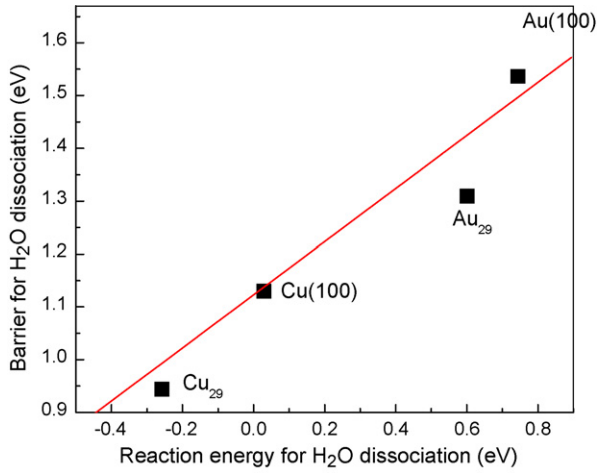

Fig. 10. Correlation between the calculated barrier ((E_a) and the calculated reaction energy ((E) for water dissociation on several copper and gold systems. The Cu and Au clusters have the structural configuration shown in Fig. 9.

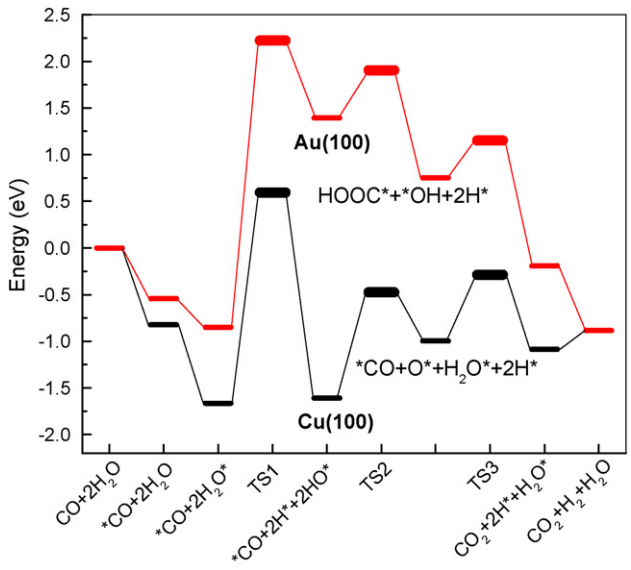

Fig. 11. DF calculated reaction profile for the WGS on Cu(1 0 0) and Au(1 0 0).

and the most energy-consuming step, or rate-limiting step, is water dissociation with a ΔE_3 of +0.06 eV and a barrier (ΔE_{a_3}) of +2.26 eV. In contrast, the dissociation of adsorbed OH* and the formation of CO_2 are more facile. All the adsorbates bond more weakly on Au(1 0 0) than on Cu(1 0 0). Consequently, the rate-limiting dissociation of H_2O on Au(1 0 0) is even more endothermic ($\Delta E_3 = +1.58$ eV) and the corresponding barrier is also higher ($\Delta E_{a_3} = +3.06$ eV). These DFT results are in agreement with our experimental measurements, which show that Cu is a good WGS catalyst while Au is an extremely poor one. The results in Fig. 11 indicate that gold will be an excellent WGS catalyst if in some way is helped with the dissociation of water. In Au/MoO_2 and Au/CeO_2, the oxide support could activate the system by helping in the dissociation of water. The metal nanoparticles probably help in the binding of CO, which reacts then with the oxide to form CO_2 gas and an O vacancy (redox mechanism) [27], or the adsorbed CO may form a carbonate- or formate-like species on the surface that will decompose into CO_2 gas and an O vacancy [28]. The key point here is that the admetal helps to keep O vacancies in the oxide surface, and these sites facilitate the most difficult step in the water–gas shift reaction: the dissociation of H_2O.

4. Conclusion

The water–gas shift (WGS, $CO + H_2O \rightarrow H_2 + CO_2$) reaction was studied on a series of gold/molybdena and copper/molybdena surfaces ($P_{CO} = 20$ Torr; $P_{H_2O} = 10$ Torr; $T = 575$–650 K). Although bulk metallic Au is inactive as a catalyst for the WGS and worthless in this respect when compared to bulk metallic Cu, Au nanoparticles supported on MoO_2 are a little bit better catalysts than Cu nanoparticles. The WGS activity of the Au and Cu nanoparticles supported on MoO_2 is five to eight times larger than that of Cu(1 0 0). The apparent activation energies are 7.2 kcal/mol for Au/MoO_2, 7.8 kcal/mol for Cu/MoO_2, and 15.2 kcal/mol for Cu(1 0 0). The Cu/MoO_2 surfaces have a catalytic activity comparable to that of Cu/CeO_2(1 1 1) surfaces and superior to that of $Cu/ZnO(0\,0\,0\,\bar{1})$ surfaces. Post-reaction surface characterization indicates that the admetals in Au/MoO_2 and Cu/MoO_2 remain in a metallic state, while there is a minor $MoO_2 \rightarrow MoO_3$ transformation. Formate- and/or carbonate-like species are present on the surface of the catalysts. DFT calculations indicate that the oxide support in Au/MoO_2 and Cu/MoO_2 is directly involved in the WGS process.

Acknowledgements

The authors are grateful to J. Hanson and W. Wen for thought provoking conversations about the behavior of Cu/MoO_2 catalysts in the WGS. The research carried out at Brookhaven National Laboratory was supported by the US Department of Energy (Chemical Sciences Division, DE-AC02-98CH10886). M. Pérez and J. Evans thank INTEVEP for a research grant that made possible part of this work.

References

[1] J.M. Thomas, W.J. Thomas, Principles and Practice of Heterogeneous Catalysis, VCH, New York, 1997.
[2] Y. Liu, Q. Fu, M. Flytzani-Stephanopoulos, Catal. Today 93–95 (2004) 241.
[3] Q. Fu, H. Saltsburg, M. Flytzani-Stephanopoulos, Science 301 (2003) 935.
[4] J.A. Rodriguez, P. Liu, J. Hrbek, J. Evans, M. Pérez, Angew. Chem. Int. 46 (2007) 1329.
[5] R. Burch, Phys. Chem. Chem. Phys. 8 (2006) 5483.
[6] B. Hammer, J.K. Nørskov, Nature 376 (1995) 238.
[7] J.A. Rodriguez, Dekker Encyclopedia of Nanoscience and Nanotechnology, Dekker, New York, 2004, pp. 1297–1304.
[8] M. Haruta, Catal. Today 36 (1997) 153.
[9] M.S. Chen, D.W. Goodman, Science 306 (2004) 252.
[10] X. Wang, J.A. Rodriguez, J.C. Hanson, M. Perez, J. Evans, J. Chem. Phys. 123 (2005) 221101.
[11] J.A. Rodriguez, G. Liu, T. Jirsak, J. Hrbek, Z. Chang, J. Dvorak, A. Maiti, J. Am. Chem. Soc. 124 (2002) 5242.
[12] L.M. Molina, B. Hammer, Appl. Catal. A: Gen. 291 (2005) 21.
[13] H. Häkkinen, S. Abbet, A. Sanchez, U. Heiz, U. Landman, Angew. Chem. Int. Ed. 42 (2003) 1297.
[14] L. Giordano, G. Pacchioni, T. Bredow, J. Fernández-Sanz, Surf. Sci. 471 (2001) 21.
[15] J.A. Rodriguez, M. Pérez, J. Evans, G. Liu, J. Hrbek, J. Chem. Phys. 122 (2005) 241101.
[16] J.A. Rodriguez, M. Pérez, T. Jirsak, J. Evans, J. Hrbek, L. González, Chem. Phys. Lett. 378 (2003) 526.
[17] M.S. Spencer, Top. Catal. 8 (1999) 259.
[18] W. Wen, L. Jing, M.G. White, N. Marinkovic, J.C. Hanson, J.A. Rodriguez, Catal. Lett. 113 (2007) 1.
[19] T. Jirsak, M. Kuhn, J.A. Rodriguez, Surf. Sci. 457 (2000) 254.
[20] C.T. Campbell, K. Daube, J. Catal. 104 (1987) 109.
[21] J. Nakamura, J.M. Campbell, C.T. Campbell, J. Chem. Soc. Faraday Trans. 86 (1990) 2725.
[22] C.V. Ovensen, P. Stoltze, J.K. Nørskov, C.T. Campbell, J. Catal. 134 (1992) 445.
[23] C.D. Wagner, W.M. Riggs, L.E. Davis, J.F. Moulder, G. Muilenberg, Handbook of X-ray Photoelectron Spectroscopy, Perkin-Elmer, Eden Praire, MN, 1977, pp. 82 and 104.

[24] L. Barrio, P. Liu, J.A. Rodriguez, J.M. Campos-Martin, J.L.G. Fierro, J. Chem. Phys. 125 (2006) 164715.
[25] P. Liu, J.A. Rodriguez, J. Chem. Phys. 126 (2007) 164705.
[26] P. Liu, J.A. Rodriguez, J.T. Muckerman, J. Hrbek, Phys. Rev. B 67 (2003) 155416.
[27] T. Bunluesin, R.J. Gorte, G.W. Graham, Appl. Catal. B: Environ. 15 (1998) 107.
[28] S. Ricote, G. Jacobs, M. Milling, Y. Ji, P.M. Patterson, B.H. Davis, Appl. Catal. A: Gen. 303 (2006) 35.